Bulgarian Chemical Communications, Volume 56, Special Issue D (pp. 121-127) 2024 DOI: 10.34049/bcc.56.D.S1P44

Synthesis and luminescence characteristics of yttrium, aluminum and lanthanum borates doped with europium ions (Eu^{3+})

K. Hristova[1]*, I. Kostova[1], T. Eftimov[2, 3], D. Tonchev[1]

[1]*University of Plovdiv "Paisii Hilendarski", Department of Chemical Technology, 24 Tsar Asen Str., Plovdiv, Bulgaria*
[2]*Centre de Recherche en Photonique, Université du Québec en Outaouais, 101 rue Saint-Jean-Bosco, Gatineau, Québec, J8X 3X7, Canada*
[3]*Central Laboratory for Applied Physics, Bulgarian Academy of Sciences, 61 Saint Petersburg Blvd, Plovdiv, Bulgaria*

Received: October 27, 2023; Revised: April 11, 2024

Inorganic materials doped with rare earth (RE) ions are an object of intense research due to their optical and electrical properties. These materials have the potential for various applications, such as solid-state lasers, active planar waveguides, optical fiber amplifiers, light-emitting diodes (LEDs), displays, ink fillers, security features, etc. RE trivalent ions can emit light from the ultraviolet (UV) to the near-infrared (NIR) regions due to electronic transitions of the *4f-5d* levels.

Yttrium borate doped with europium ions was prepared by solid-state synthesis in a muffle furnace at 900°C for 4 hours, while lanthanum and aluminum borates doped with europium ions were prepared at 1000°C for 6 hours again in a muffle furnace. The resulting materials are fine white powders. Among the rare earth ions, europium is one of the most commonly used activators because the ions of Eu^{3+} and Eu^{2+} can be used as emission sites in the host lattices. Eu^{3+} ions can produce effective sharp emission peaks in different matrix compositions. Photoluminescence analysis of the samples was performed, based on which the luminescence intensity of the Eu^{3+} ion was determined through a comparative characteristic. $YBO_3:Eu^{3+}$ phosphor is optically active and chemically stable. It is characterized by a strong orange-red emission at ≈ 591 nm, ≈ 612 and ≈ 696 nm due to the $^5D_0 \rightarrow {}^7F_1$ and $^5D_0 \rightarrow {}^7F_2$ electronic transitions, respectively. Red emission is also observed for $LaBO_3:Eu^{3+}$ at ≈ 592 and ≈ 615 nm, characterizing the $^5D_0 \rightarrow {}^7F_1$ and $^5D_0 \rightarrow {}^7F_j$ (j=0, 1, 2, 3, 4) transitions. While aluminum borate doped with europium ion shows intense emission at ≈ 612 nm, making this material suitable for lighting devices. The technique of Fourier transform infrared spectroscopy (FTIR) was used to study the structure of the obtained materials.

Keywords: Europium ion, solid-state reaction, fluorescence analysis, rare earth borates, aluminum borate, red emission.

INTRODUCTION

Rare earth elements are widely used as luminescent materials in various fields of practice. These materials are indispensable in the production of fluorescent lamps, scintillators, lasers, diodes, etc. [1, 2]. Of importance among them is europium, which in the +3 oxidation state is one of the most interesting and applicable elements. Upon irradiation with an ultraviolet source, the trivalent europium ion exhibits intense red fluorescence due to various electronic transitions [3]. This photoluminescence is observed not only for Eu^{3+} ions doped in crystalline inorganic matrices or glasses but also for europium (III) complexes with organic ligands. These ligands can act as a source to absorb the excitation light and to transfer the excitation energy to the higher energy levels of Eu^{3+} ion, where the emitting excited levels can be populated [4]. The lines of the emission spectra are usually sharp and depend on the crystal field around the metal ions [5]. In this work we synthesized different borates, which are optically apparent up to 140–180 nm, therefore, the UV light can openly excite impurity activator in such kind of host lattice. The energy transmission from a borate host crystal excited by UV light to the trivalent rare-earth activators leads to host-excited luminescence. The doping with europium ion in various matrices yields luminescent materials for biochemical or biomedical applications [6]. Europium ions have interesting optical characteristics such as well-defined spectral lines and red/orange emission, which have been used for technological applications in displays, lamps, etc. [7]. Most of the standard commercial red phosphors are based on Eu^{3+}-doped oxides. With an appropriate selection of the matrix, it is possible to use low concentrations of the activating ion and achieve high fluorescence intensity [8]. An interesting and very important application of europium as a main component is in the anti-counterfeiting ink of banknotes, as well as QR codes [9].

The aim of the present work is to study the influence of different inorganic matrices - yttrium, lanthanum and aluminum borates, on the activation

* To whom all correspondence should be sent:
E-mail: *katyahristova@uni-plovdiv.bg*

of europium 3+ (Eu^{3+}) ion after establishing optimal synthesis conditions in terms of temperature and duration [10, 11]. By means of photoluminescence analysis, a comparative characterization of the influence of these factors on the luminescence intensity of the Eu^{3+} ion was performed. The technique of Fourier transform infrared spectroscopy (FTIR) was used to study the structure of the obtained materials.

EXPERIMENTAL

Materials

For the synthesis of luminescent materials, the following reagents of analytical grade purity were used: Y_2O_3 (yttrium (III) oxide, 99.99 % (trace metal basis), CAS: 1314-36-9, Acros organics); H_3BO_3 (boric acid, 99%, Index # 005-007022-2); Eu_2O_3 (europium (III) oxide, 99.99% (trace metal basis), Acros, CAS: 1308-96-9), La_2O_3 (lanthanum (III) oxide, 99.9%), Al_2O_3 (aluminum oxide for chromatographic purposes 99%), purchased from Alfa Aesar.

Sample preparation

For the synthesis of materials, the necessary quantities of the starting substances were stoichiometrically calculated for 1 gram of sample, as shown in equations (1), (2), (3).

$$Y_2O_3 + 2\ H_3BO_3 \longrightarrow 2\ YBO_3 + 3\ H_2O \quad (1)$$

$$La_2O_3 + 2\ H_3BO_3 \longrightarrow 2\ LaBO_3 + 3\ H_2O \quad (2)$$

$$Al_2O_3 + 2\ H_3BO_3 \longrightarrow 2\ AlBO_3 + 3\ H_2O \quad (3)$$

Description of sample composition is given in Table 1. The solid-state synthesis was carried out in a muffle furnace LM 312.07 with a G400 controller with a temperature range of 0-1200°C. Sample S29 SS was prepared by mixing stoichiometric amounts of Y_2O_3 and excess of H_3BO_3 45% as shown in equation (1) with 2 mol % Eu_2O_3 as doping agent at 900°C for 4 hours at a heating rate of 15°C/min. For samples S60 SS and S70 SS, the synthesis was carried out again in a muffle furnace at temperature of 1000°C for 6 hours, with a heating rate of 15°C/min by mixing stoichiometric amounts of the starting substances - La_2O_3/Al_2O_3, H_3BO_3 - 45% excess and 2 mol % Eu_2O_3 as shown in equations (2) and (3). The reagents were weighed, mixed, and well-homogenized. The prepared mixtures were placed in porcelain crucibles and heated. After 4 hours for sample S29 SS and 6 hours for S60 SS and S70 SS, they were left in the furnace and slowly cooled for 16 hours.

Photoluminescence measurements

The photoluminescence spectra were measured at room temperature by an Ocean Optics fiber optic QEB1104 spectrometer in the range 200–990 nm and a combination of an Energetic Laser driven white light source (190 nm – 2500 nm) and a fiber-optic monochromator (MonoScan 2000, Ocean Optics). The main advantage of this scheme is that it minimizes reflection from the samples and maximizes the luminescence spectrum. The synthesized samples are fine white powders, which makes them suitable for fillers in polymers, paper, inks, etc.

Fourier transform-infrared (FTIR) spectroscopy

FTIR Bruker Vertex 70 spectrometer was used for the FTIR analyses, which provided peak sensitivity in the MIR 4000-400 cm^{-1} region. The IR data were analyzed to compile the structure spectra, and to get information about the interatomic forces and the reasons for the appearance of the different types of structures in the rare earth borates.

RESULTS AND DISCUSSION

It was found that temperature of synthesis affects the substitution of the activator, that is, the europium ion can replace yttrium, aluminum, or lanthanum ion in the host lattice. This occurs when the ionic radii of the activator and the host are sufficiently different. It is known that replacing Eu^{3+} with Y^{3+} results in a larger unit cell volume due to the difference in radii (0.95 and 0.90 Å, respectively) [12]. The same can be said for lanthanum, whose ionic radius is 1.06 Å, and for aluminum – 0.54 Å [13, 14]. From the observed excitation-emission scan of the sample S29 SS, the most intense emission peaks are at ≈ 591 nm (2.10 eV) (orange region) due to the $^5D_0 \rightarrow {}^7F_1$ transition, ≈ 612 nm (2.03 eV) (red) corresponding to the $^5D_0 \rightarrow {}^7F_2$ transition and 696 nm (1.78 eV) due to $^5D_0 \rightarrow {}^7F_4$ as shown in Fig. 1(a and b). Very intense and hypersensitive transition $^5D_0 \rightarrow {}^7F_2$ indicates that Eu^{3+} is not on a site with a center of symmetry [15, 16]. For the S_6 symmetry, which has an inversion center, the rule forbids an electron-dipole transition within the 4f subshells. This transition is allowed only under the condition that the europium ion occupies a site without an inversion center and is sensitive to local symmetry.

Table 1. Description of sample composition

Samples	Y_2O_3 (g)	La_2O_3 (g)	Al_2O_3 (g)	H_3BO_3 excess %	H_3BO_3 (g)	Eu_2O_3 (mol %)	Eu_2O_3 (g)
S29 SS	0.7850			45	0.6232	2	0.007
S60 SS		0.7249		45	0.3987	2	0.007
S70 SS			0.4519	45	0.7946	2	0.007

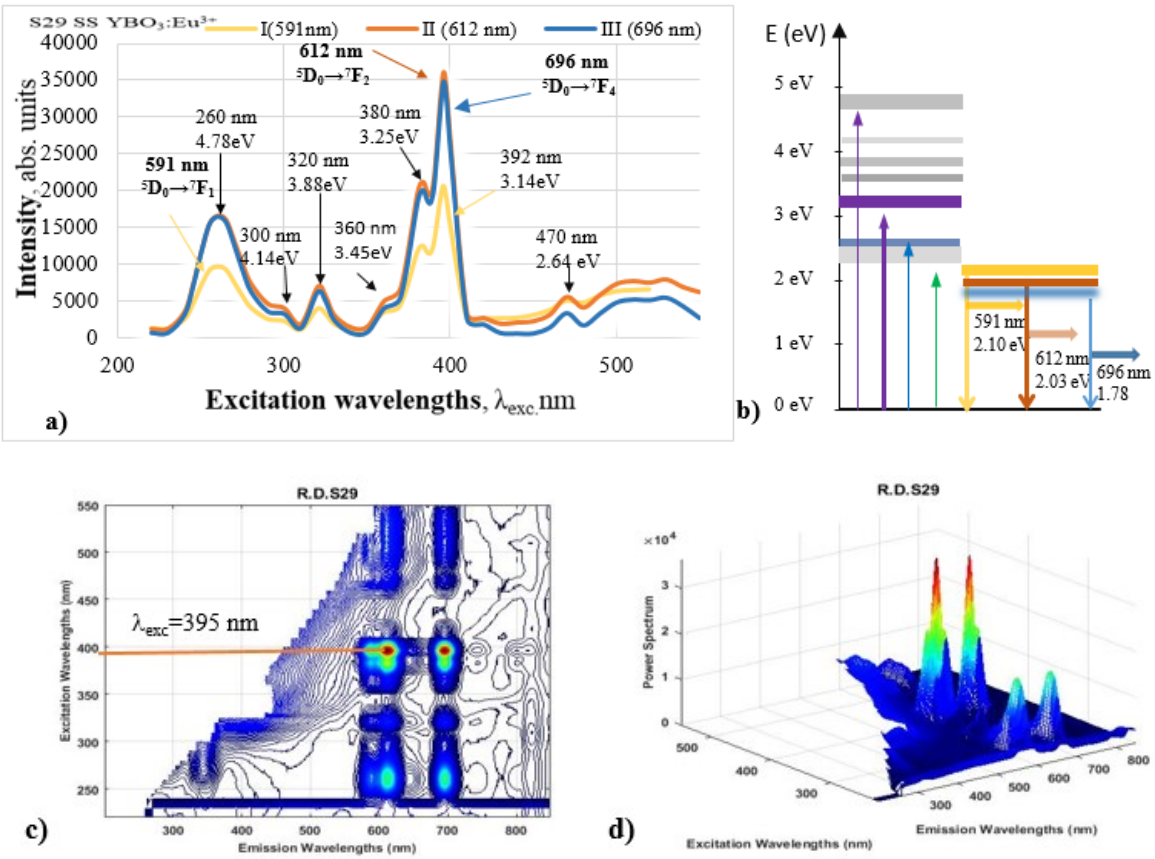

Fig. 1. a) Graphic representation of the emission intensity at 591 nm, 612 nm and 696 nm *vs*. excitation wavelength; **b)** corresponding energy levels of yttrium borate doped with Eu^{3+}; **c)** excitation-emission 3D spectra of $YBO_3:Eu^{3+}$ topographic representation; **d)** side view presentation.

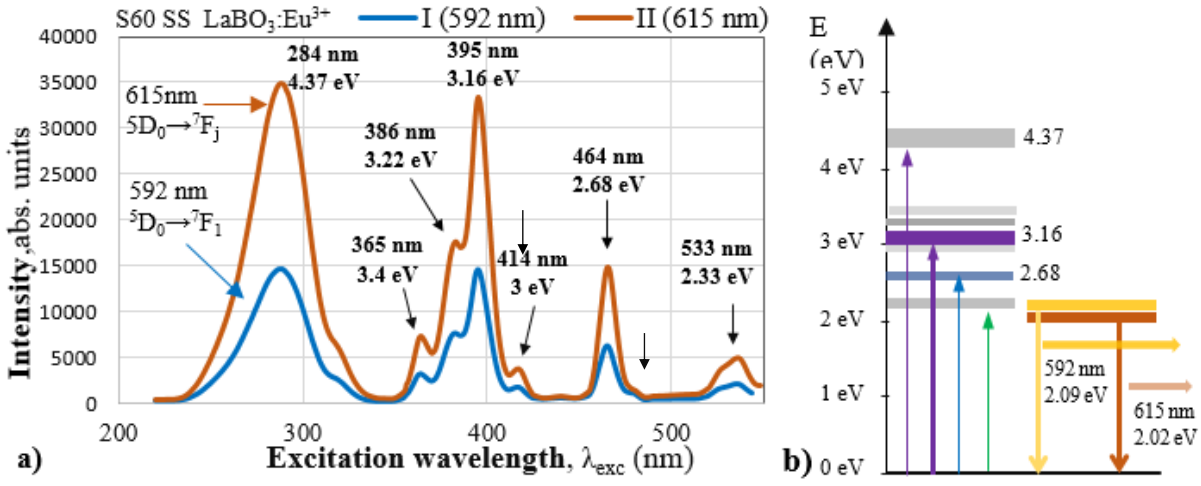

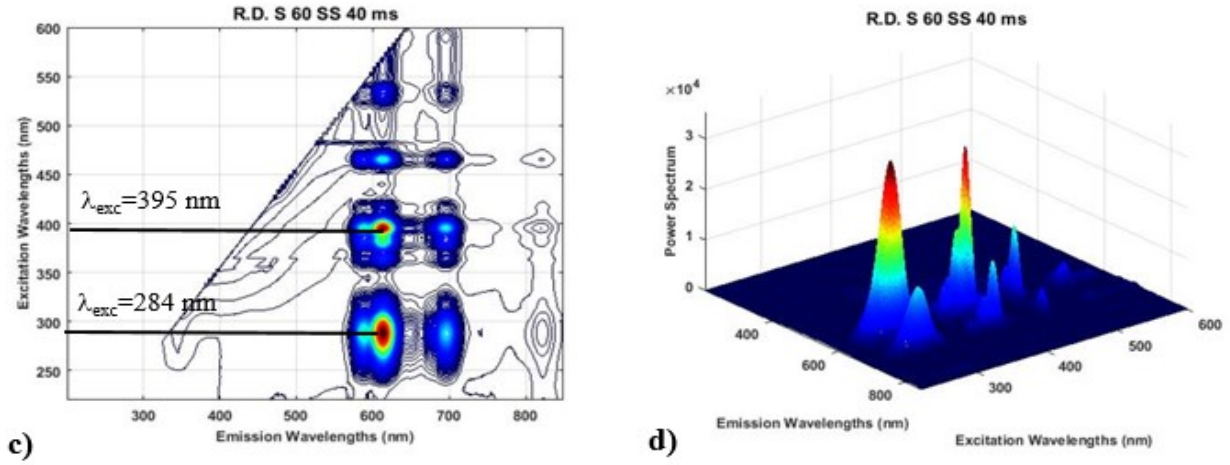

Fig. 2. a) Graphic representation of the emission intensities at 592 nm and 615 nm on the excitation wavelength; **b)** energy levels (eV) of lanthanum borate doped with europium ion; **c)** 3D excitation-emission spectra of $LaBO_3$: Eu^{3+}: topographic presentation; **d)** side view

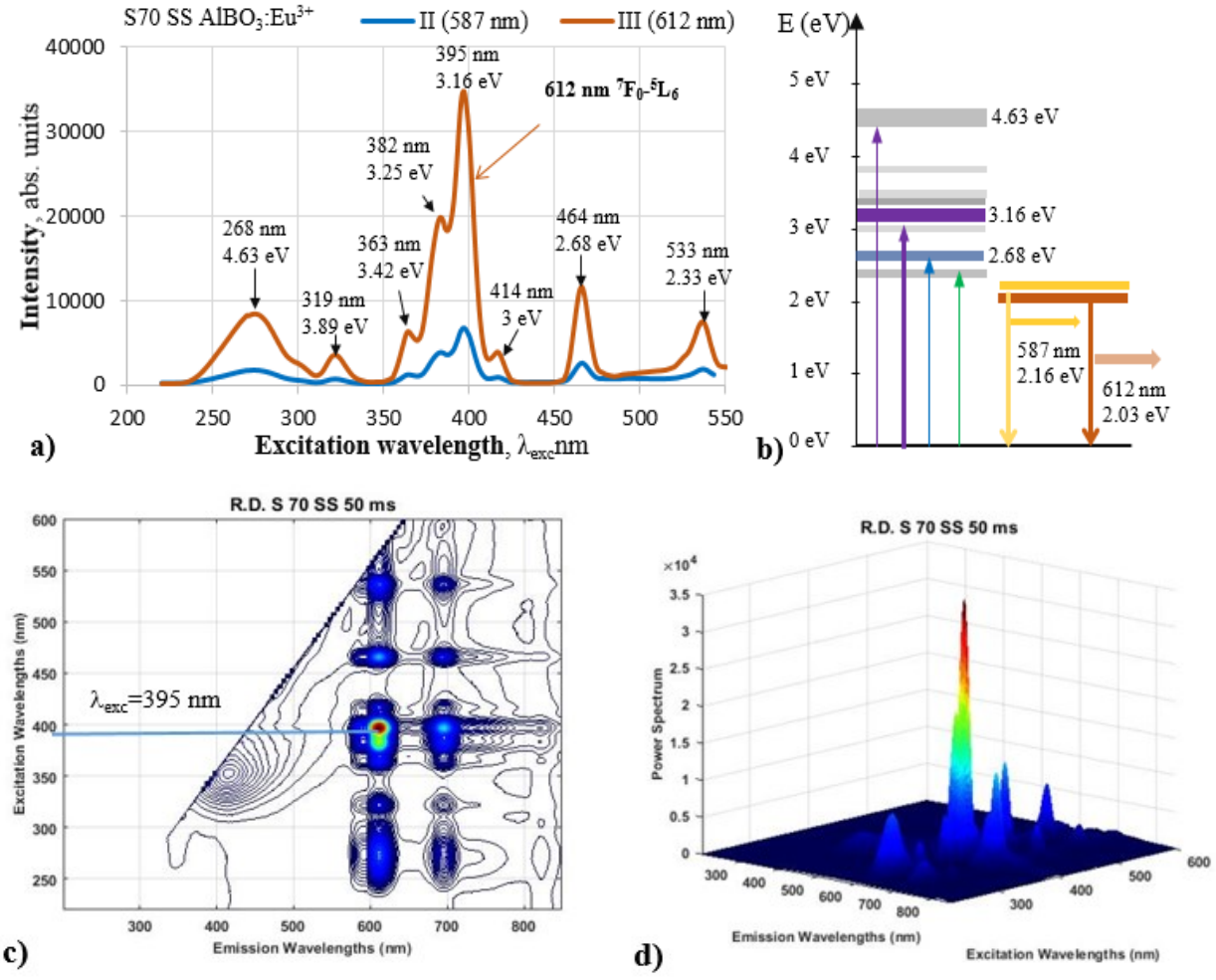

Fig. 3. a) Graphic representation of the emission intensity at 587 nm and 612 nm on the excitation wavelength; **b)** energy levels (in eV) of aluminum borate doped with europium ion. Eu^{3+}: **c)** 3D excitation-emission graph of $AlBO_3$: topographic representation; **d)** side view.

When Eu^{3+} ions occupy sites of inversion centers, the $^5D_0 \rightarrow {}^7F_1$ transitions should be relatively strong and the $^5D_0 \rightarrow {}^7F_2$ transitions should be relatively weak [17]. In our case, we observed the opposite statement and concluded that the europium ion isn't at the site with the center of inversion for 284 nm (4.37 eV) with emission at ≈ 592 nm (orange region) due to the $^5D_0 \rightarrow {}^7F_1$ transition and with emission at ≈ 615 nm (2.02 eV) due to the $^5D_0 \rightarrow {}^7F_j$ transition (red region). In the excitation source of 395 nm we observed emission at 595 and 615 nm and the weakest fluorescence upon excitation at 464 nm (2.68 eV) again 615 nm (red), as shown in Fig. 2a) and b). The peaks at 615 nm correspond to $^5D_0$–^7F_j transitions between multiplets (j = 0, 1, 2, 3, 4) characteristic of the Eu^{3+} ion as shown at Fig. 2(a and b) [18]. For an excitation at $\lambda_{max} \approx 290$ nm, excitation energy transferred from the 2p orbital of the O^{2-} to the–4f of Eu^{3+} is observed, the energy of which depends on the stability of the fields of the surrounding O^{2-} ions. The peaks in the range 350–430 nm (365, 386 nm) (3.40, 3.22 eV) correspond to transitions of Eu^{3+} f–f electrons from the ground state $^7F_0$ to the excited levels $^5D_4$, $^5L_6$ и $^5G_{4,5}$ [19]. In the excitation spectra, the charge transfer is much more intense when in the matrix the alloying element is the europium ion as shown in Fig. 2c) and d) [5]. The displacement of the charge transfer peaks to longer wavelengths may also be caused by a decrease in the distance between Eu^{3+} and O^{2-} and therefore a decrease in the electronegativity difference between the ions [20]. Aluminum borate is characterized by highly efficient radiation in the visible region. Upon excitation with 395 nm, emission at 612 nm was observed, corresponding to the $^7F_0$-$^5L_6$ transition characteristic of the europium ion in the aluminum borate matrix and which is the most intensive peak [21]. Typical emission from $^5D_0$ to $^7F_{0,\,1,\,2,\,3,\,4}$ was measured in the range of 276-536 nm as shown in Fig. 3a and b [22]. An important feature observed in the emission spectra is that when considering all the transitions from $^5D_0$ to $^7F_{0,\,1,\,2,\,3,\,4,}$ peak broadening takes place [23]. This can be attributed to the distribution effect of the different microenvironments around Eu^{3+}, i.e. separate symmetry sites occupied by Eu^{3+} in the host lead to inhomogeneous broadening. When the $AlBO_3$ host consists of octahedra, it can be assumed that Eu^{3+} replaces Al^{3+} in the octahedral sites. The magnetic dipole character of $^5D_0 \rightarrow {}^7F_1$ makes it possible to determine the intensity parameters of the emission spectrum since this transition does not depend on the local ligand field and can be used as a reference for the entire spectrum.

FTIR analysis

Depending on the size of the cations, rare earth borates crystallize in 3 spatial structures – vaterite, calcite, and aragonite [24]. It is believed that the vibrational spectra of vaterite-type orthoborates significantly differ from calcite and aragonite types. Borate compounds of vaterite type are characterized by extremely broad and intense absorption peaks in the range from 800 cm^{-1} to 1200 cm^{-1}. These peaks can be attributed to the vibration of the $B_3O_9^{9-}$ groups in the vaterite-type orthoborates. For the isolated XO_3 (X=yttrium, lanthanum, aluminum) planar ion having trigonal symmetry, there are four main modes of vibration: symmetric stretching v_1, out-of-plane bending v_2, doubly degenerate antisymmetric stretching v_3, and doubly degenerate antisymmetric planar bending, v_4 [25]. Of these, three are active in the infrared region, while v_1, a symmetric stretch, is inactive in isolated ions. In a crystalline solid containing more than one molecule per unit cell, symmetry considerations indicate that all modes can be active and coupling between different modes can even eliminate degeneracies [26, 27]. Six bands are expected in aragonite because in this structure v_1 is active and degeneracies have been removed from v_3 and v_4. Vaterite is known to possess a hexagonal structure containing two or more molecules per unit cell [28-30].

For the sample S29 SS, (Fig. 4, S29 SS), the weak peak at 570 cm^{-1} is attributed to in-plane bending of the BO_4 group or the BO_3 group in vaterite-type orthoborates [31]. The bending vibrations of the B–O–B bond in the borate network are located at 710 cm^{-1}. In the range 731 – 873 cm^{-1} the YBO_3 vibrations appear. The peaks located in the region from 916 cm^{-1} to 1250 cm^{-1} are due to B-O symmetric stretching vibrations of the bond in BO_4 units of diborate and tetraborate groups [32]. B–O stretching vibrations are best expressed at 1250 cm^{-1} [33]. The intense peak at 1270 cm^{-1} corresponds to the B–O stretching vibration in BO_3 units of various types of borate groups appearing in the weaker band at 1381 cm^{-1} [34]. The peak at 1409 cm^{-1} represents the stretching vibrations of the B–O bonds for the tetrahedral BO_4 groups [35]. The band centered at 1463 cm^{-1} corresponds to B-O_{sym} symmetric stretching of BO_3 in ortho-borate groups [36]. The most intense peak at 1724 cm^{-1} is due to pentaborate arising from the B – O stretching vibration of $[BO_3]^{3-}$ [31]. Data from the IR spectrum of the lanthanum borate are shown in Fig. 4, S60 SS. The IR spectrum of $LaBO_3$ doped with Eu^{3+} shows strong absorption peaks in the range 1269–592 cm^{-1}, inherent to the vibrations of planar trigonal $[BO_3]^{3-}$ groups [37-40]. Two weak absorption bands at 592 and 611 cm^{-1} are

due to in-plane (ν_4) and the strong peak at 714 cm^{-1} is due to out-of-plane (ν_2) B–O-B bending modes. The peak at 940 cm^{-1} (ν_1) refers to the symmetric stretching of the three-coordinate bands [$\nu_s(B_{(3)}–O)$] modes of the $[BO_3]^{3-}$ groups. The most intense and sharp peak appears at 1269 cm^{-1}, which is characteristic of the B-O asymmetric stretching of BO_3 [20]. For aluminum borates doped with europium ion, the weak peak observed in the range of 448–505 cm^{-1} is attributed to the bending of BO_4 units as shown in Fig. 4, S70 SS. The peak at 547 cm^{-1} is attributed to the formation of Eu^{3+} borate. The following are bands that correspond to the different phases and stretching modes: 648 cm^{-1} B-O-B in BO_3 [36]. The band at 717 cm^{-1} for the formation of the B_2O_3 glassy body due to the bending vibration of the B–O–B bond in the borate network was determined. The stretching vibration of Al–O in AlO_4 appears at 780 cm^{-1}[37]. The bands in the range of 884–1052 cm^{-1} can be assigned to B–O bond stretching vibration in BO_4 units of di-, tri-, tetra- and penta-borate groups as shown in [40 Fig. 6.]. The band at 1437 cm^{-1} corresponds to B–O asymmetric stretching vibrations in BO_3 units.

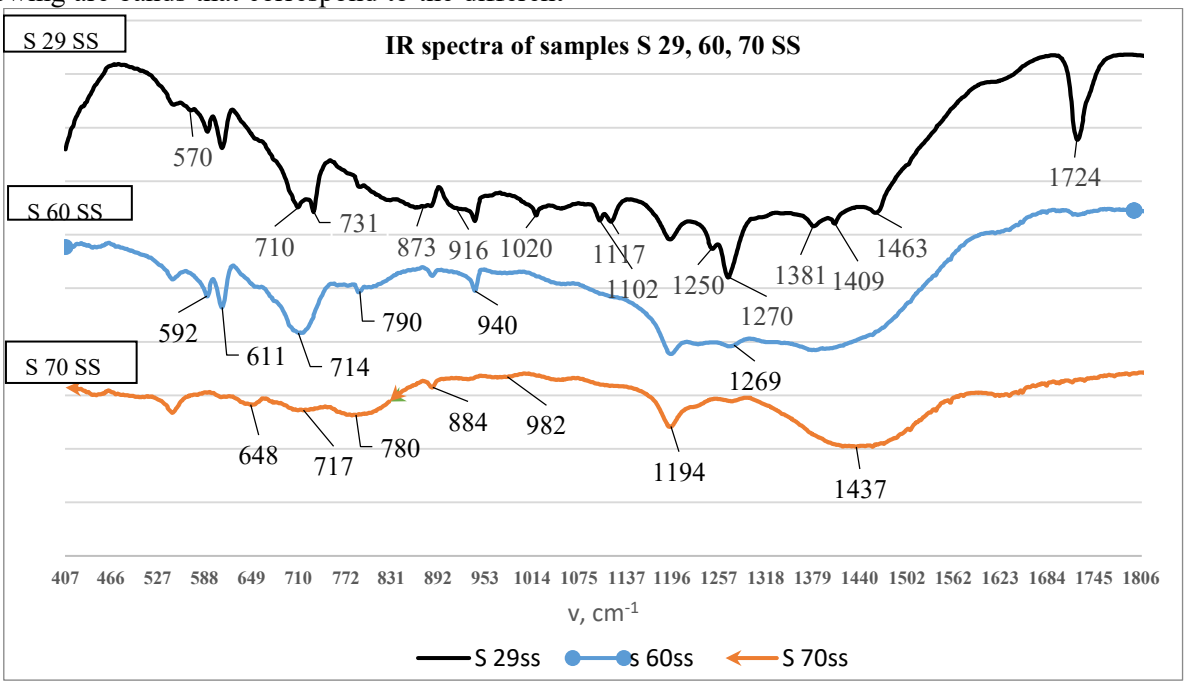

Fig. 4. FTIR spectra of yttrium, lanthanum and aluminum borates doped with europium ion.

CONCLUSION

Three samples with different matrix compositions - YBO_3, $LaBO_3$, and $AlBO_3$ doped with europium oxide were synthesized by a solid-state reaction. The samples were analyzed with a spectrometer to establish the highest emission intensity resulting from europium ion activation in the different matrices. The excitation spectra of the obtained materials show transitions from $^5D_0$ to $^7F_1$ $^7F_2$ $^7F_3$ and $^7F_4$ states. When comparing the spectra of aluminum, lanthanum, and yttrium borate, for excitation at ≈ 284 nm, only europium-doped lanthanum borate produces an intense peak with emission at 615 nm. Two intense peaks are also observed in the yttrium borate matrix, which, under the excitation with ≈ 395 nm, emit at ≈ 612 and 696 nm, respectively, due to different electronic transitions. For the aluminum borate matrix, upon excitation with ≈ 290 nm, an extremely weak, undetectable fluorescence is observed at 590 nm, the most intense peak for this matrix is at 612 nm when the excitation source is ≈ 395 nm. It was found that the matrix with yttrium borate, europium ion is well activated and gives peaks in the orange and red region of the spectrum, for the matrix with lanthanum borate two strong peaks are observed in the red region, but when irradiated with sources of different wavelength, for the aluminum borate matrix we observe one intense peak in the red region. Based on these studies, depending on the target product, a suitable matrix can be selected for different areas of application. Of the lanthanide group, europium oxide itself has fluorescence in the red region. FTIR spectra evidence the presence of BO_4 vibrations, B–O deformation mode, and stretching vibrations of BO_4 units in tri-, tetra, and penta-borate groups in all RE-doped materials, absorption peaks arise due to electronic transition between inner orbitals. The addition of rare earth

oxide to different matrices leads to the activation of the europium ion and a shift of the absorption peaks.

REFERENCES

1. M. V. Nazarov, J. H. Kang, D. Y. Jeon, S. Bukesov, T. Akmaeva, *Optical Materials,* **27**, 1587 (2005).
2. R. Srinivasan, N. R. Yogamalar, J. Elanchezhiyan, R. J. Joseyphus, A. C. Bose, *Journal of Alloys and Compounds,* **496** (1-2), 472 (2010).
3. H. Qi, Z. Zhao, G. Zhan, B. Sun, W. Yan, C. Wang, L. Wang, Z. Liu, Z. Bian, C. Huang, *Inorg. Chem. Front.*, (2020), doi: 10.1039/D0QI00762E
4. Poonam, S. P. Khatkar, R. Kumar, Avni Khatkar, V. B. Taxak *Journal of Materials Science: Materials in Electronics,* (2015) doi:10.1007/s10854-015-3330-7
5. M. V. Nazarov, J. H. Kang, D. Y. Jeon, E. J. Popovici, L. Muresan, B. S. Tsukerblat, *Solid State Communications,* **133**, 183 (2005).
6. R. L. Kohale, V. B. Pawade, A. H. Deshmukh, *Electronic and Optical Materials* (2021).
7. A. K. Gangwar, K. Nagpal, P. Kumar, N. Singh, B. K. Gupta, Bipin. *J. Appl. Phys.* **125,** 074903 (2019)
8. M. J. Q. Lauro, F. F. M. Fausto *Nanocomposites for Photonic and Electronic Applications,* **31–44** (2020), doi:10.1016/B978-0-12-818396 0.00002 9
9. D. J. Kim, S. H. Hyun, S. G. Kim; M. Yashima, *J. Am. Ceram. Soc,* **77** (2), 597 (1994).
10. E. A. Tkachenko, R. Mahiou, G. Chadeyron, D. Boyer, P. P. Fedorov, S. V. Kuznetsov, *Russian Journal of Inorganic Chemistry*, **52**(6), 829 (2007).
11. K. Hristova, S. Nachkova, Al. Peltekov, Zh. Simeonova, I. Kostova, *Technics, Technologies, Education. Safety,* **2**, 128 (2021).
12. A. A. Al-Juaid, M. A. Gabal; *Journal of Materials Research and Technology,* **14**, 10 (2021).
13. K. Chandra, V. Singh, S. K. Sharma, P. K. Kulriya, **937** 168311 (2023), doi: 10.1016/j.jallcom.2022.168311
14. J. H. Lin, S. Zhou, L. Q. Yang, G. Q. Yao, M. Z. Su, *Journal of Solid State Chem*., **134**(1), 158 (1997).
15. K. Binnemans, *Coordination Chemistry Reviews,* **295**, 1 *(2015)* doi: 10.1016/j.ccr.2015.02.015
16. N. C. Chang, *J. Appl. Phys*., **34**, 3500 (1963) doi: 10.1063/1.1729247
17. S. Sari, F. T. Senberber, M. Yildirim, A. S. Kipcak, S. A. Yuksel, E. M. Derun, *Materials Chemistry and Physics*, **200,** 196 (2017) doi: 10.1016/j.matchemphys.2017.07.056
18. N. V. Klassen, S. Z. Shmurak, I. M. Shmyt'ko, G. K. Strukova, S. E. Derenzo, M. J. Weber, *Nuclear Instruments and Methods in Physics Research A,* **537,** 144 (2005).
19. N. I. Steblevskaya, M. V. Belobeletskaya, M. A. Medkov. *Russian Journal of Inorganic Chemistry*, **66**, 468 (2021)
20. P. J. Yadav, N. D. Meshram, S. V. Maharil. *Optical Materials*: X, **19**, 100252 (2023).
21. S. P. Ray, *J. Am. Ceram. Soc,* **75(9)**, 2605 (1992).
22. A. S. Kipcak, D. Y. Baysoy, E. Derun, S. Piskin, *Advances in Materials Science and Engineering*, **1-9** (2013).
23. R. Srinivasan, N. R. Yogamalar, J. Elanchezhiyan, R. J. Joseyphus, A. C. Bose, *Journal of Alloys and Compounds,* **496**(1-2), 1 (2010).
24. G. Hertzberg, Molecular spectra and molecular structure, vol II, 7th edn. D. van Nostrand Co, **178,** ,\N.Y.,1956.
25. C. E. Weir, E. R. Lippincott, *J. Res. Natl. Bur. Stand. A, Phys. Chem.,* **65**A(3), 173 (1961).
26. R. S. Halford, *The Journal of Chemical Physics,* **14**, 395 (1946), doi: 10.1063/1.1724158
27. R. W. G. Wykoff, The Chemical Catalog Co, 2nd edn., **80**, N.Y., 1931.
28. H. J. Meyer. *Angew. Chem.,* **71,** 678, (1959).
29. L. H. Ahrens, *Geochim. Cosmochim. Acta,* 155 (1952) doi:10.1016/0016-7037(52)90004-5
30. A. G. Christy, *Crystal Growth & Design, acs.cgd.7b00481* (2017). doi: 10.1021/acs.cgd.7b00481
31. V. Hegde, N. Chauhan, V. Kumar, C. S. D. Viswanath, K. K Mahato, S. D. Kamath, *Journal of Luminescence*, (2018) doi: org/10.1016/j.jlumin.2018.11.023
32. A. Y. Madkhli, Ü. H. Kaynar, M. B. Coban, M. Ayvacikli, A. Canimoglu, N. Can, *Materials Research Bulletin,* **161** (2023). https://doi.org/10.1016/j.materresbull.2023.112167
33. P. Pascuta, S. Rada, G. Borodi, M. Bosca, L. Pop, E. Culea, *Journal of Molecular Structure,* **924–926,** 214 (2009).
34. P. O. Ike, A. C. Nwanya, K. K. Agwu, F. I. Ezema. *Optical Materials,* **127**, 112263 (2022) https://doi.org/10.1016/j.optmat.2022.112263
35. A. S. Oreshonkov, E. M. Roginskii, N. P. Shestakov, I. A. Gudim, V. L. Temerov, I. V. Nemtsev, M. S. Molokeev, S. V. Adichtchev, A. M. Pugachev, Y. G. Denisenko, *Materials,* **13** (3) 545 (2020).
36. A. Szczeszak, K. Kubasiewicz, S. Lis, *Optical Materials,* **35(**6), 1297 (2013).
37. N. I. Steblevskaya, M. A. Medkov, M. V. Belobeletskaya, RF Patent 2651028, *Russian Journal of Inorganic Chemistry,* Publ. 11 (2017).
38. C. Badan, O. Esenturk, A. Yilmaz, *Solid State Sciences,* **14**(11-12), 1710 (2012).
39. G. Heymann, T. Soltner, H. Huppertz, *Solid State Sci*. **8**, 827 (2006).
40. P. Su. Wong, M. H. Wan, R. Hussin, H. O. Lintang, S. Endud, *Journal of Rare Earths,* **32**(7), 585 (2014).